OXFORD

Human Molecular Genetics, 2016, Vol. 25, No. 23 5167–5177

doi: 10.1093/hmg/ddw331
Advance Access Publication Date: 23 October 2016
Original Article

ORIGINAL ARTICLE

Myeloid cells are capable of synthesizing aldosterone to exacerbate damage in muscular dystrophy

Jessica A. Chadwick[1], Sarah A. Swager[1], Jeovanna Lowe[1], Steven S. Welc[2], James G. Tidball[2], Celso E. Gomez-Sanchez[3], Elise P. Gomez-Sanchez[4] and Jill A. Rafael-Fortney[1,*]

[1]Department of Physiology and Cell Biology, College of Medicine, The Ohio State University, Columbus, OH, USA, [2]Department of Integrative Biology and Physiology, University of California Los Angeles, Los Angeles, CA, USA, [3]Department of Internal Medicine and [4]Department of Pharmacology and Toxicology, University of Mississippi Medical Center, Jackson, MS, USA

*To whom correspondence should be addressed at: Jill A. Rafael-Fortney, Ph.D., Department of Physiology & Cell Biology, The Ohio State University College of Medicine, 410 Hamilton Hall, 1645 Neil Avenue, Columbus, OH 43210, USA. Tel: (614) 292-7043; Email: rafael-fortney.1@osu.edu

Abstract

FDA-approved mineralocorticoid receptor (MR) antagonists are used to treat heart failure. We have recently demonstrated efficacy of MR antagonists for skeletal muscles in addition to heart in Duchenne muscular dystrophy mouse models and that mineralocorticoid receptors are present and functional in skeletal muscles. The goal of this study was to elucidate the underlying mechanisms of MR antagonist efficacy on dystrophic skeletal muscles. We demonstrate for the first time that infiltrating myeloid cells clustered in damaged areas of dystrophic skeletal muscles have the capacity to produce the natural ligand of MR, aldosterone, which in excess is known to exacerbate tissue damage. Aldosterone synthase protein levels are increased in leukocytes isolated from dystrophic muscles compared with controls and local aldosterone levels in dystrophic skeletal muscles are increased, despite normal circulating levels. All genes encoding enzymes in the pathway for aldosterone synthesis are expressed in muscle-derived leukocytes. 11β-HSD2, the enzyme that inactivates glucocorticoids to increase MR selectivity for aldosterone, is also increased in dystrophic muscle tissues. These results, together with the demonstrated preclinical efficacy of antagonists, suggest MR activation is in excess of physiological need and likely contributes to the pathology of muscular dystrophy. This study provides new mechanistic insight into the known contribution of myeloid cells to muscular dystrophy pathology. This first report of myeloid cells having the capacity to produce aldosterone may have implications for a wide variety of acute injuries and chronic diseases with inflammation where MR antagonists may be therapeutic.

Introduction

Duchenne muscular dystrophy (DMD) is a genetic disorder that affects approximately 1 in 5,000 boys (1). Patients have severe muscle degeneration, use a wheelchair by their early teens and have an average lifespan of only 25 years (2). We previously showed a combined treatment with the angiotensin converting enzyme (ACE) inhibitor lisinopril and mineralocorticoid receptor (MR) antagonist spironolactone reduces ongoing skeletal muscle damage and improves muscle function in a DMD mouse model (3). Spironolactone and lisinopril target the mineralocorticoid receptor directly and indirectly, respectively, through the renin-angiotensin-aldosterone system.

The mineralocorticoid receptor (MR) is a member of the nuclear hormone receptor superfamily (4). Upon hormone binding,

Received: July 12, 2016. **Revised:** August 29, 2016. **Accepted:** September 26, 2016

MR dissociates from chaperone proteins in the cytosol, forms a homodimer and translocates to the nucleus where it directs transcription of target genes (5). MR is most commonly activated by the mineralocorticoid aldosterone, but can also be activated by glucocorticoids (cortisol in humans, corticosterone in mice), because of its strong homology with glucocorticoid receptor (6,7). MR selectivity for aldosterone is largely dependent on type 2 11β-hydroxysteroid dehydrogenase (11β-HSD2) that converts glucocorticoids to inactive metabolites unable to bind MR (7).

Spironolactone binds and directly inhibits MR activation (8). Lisinopril indirectly affects MR activation by blocking the formation of angiotensin II, which normally stimulates aldosterone production (9). Treatment with lisinopril alone improves histopathology, but cannot recapitulate improvements in skeletal muscle function of dystrophic mice after combined treatment with spironolactone (3,10). We have shown that MR is present in both mouse and human skeletal muscle fibres (11). Treatment of normal human myotubes with aldosterone results in a large number of gene expression changes, supporting MR functions as a nuclear hormone receptor in skeletal muscles (11), but its function in skeletal muscle has not been investigated.

Excessive MR activation contributes to heart failure. Both the RALES (Random Aldactone Evaluation Study) and EPHESUS (Eplerenone Post-MI Heart Failure Efficacy and Survival Study) clinical trials demonstrated that the addition of an MR antagonist to standard-of-care ACE inhibitor regimens improves morbidity and mortality in patients, even when circulating aldosterone levels are within the physiological range (12,13). These studies led to several hypotheses for why MR is inappropriately activated in heart failure, including low 11β-HSD2 activity that results in glucocorticoid-mediated MR activation (14,15), and local aldosterone synthesis in the heart (16). Most aldosterone is synthesized in the adrenal cortex, but a growing body of evidence shows both aldosterone and glucocorticoids can be synthesized locally in extra-adrenal tissues, particularly in pathological states (17–23). Previous studies have demonstrated that expression of CYP11B2 or aldosterone synthase, the key enzyme in aldosterone synthesis is up-regulated in the failing heart and that cardiomyocytes can produce aldosterone *in vitro* (24–27).

The purpose of this study was to begin to elucidate the mechanism behind the efficacy of MR antagonists in dystrophic muscles. To define potential mechanisms of MR activation in skeletal muscles we investigated whether: skeletal muscle is an aldosterone selective tissue, corticosteroid levels are increased in dystrophic muscles, and local aldosterone synthesis is possible in skeletal muscle tissues.

Results

11β-HSD2 expression suggests MR selectivity for aldosterone in skeletal muscles

11β-HSD2 is an enzyme expressed in specific cell types that regulates MR selectivity for aldosterone by converting glucocorticoids to inactive metabolites (7). 11β-HSD2 has never been investigated in skeletal muscle. However, our previous study demonstrated that treatment of cultured myotubes with aldosterone results in numerous gene expression changes, which supports aldosterone-dependent activation of MR in skeletal muscle is possible (11). To determine whether skeletal muscle is an aldosterone selective tissue, we investigated whether

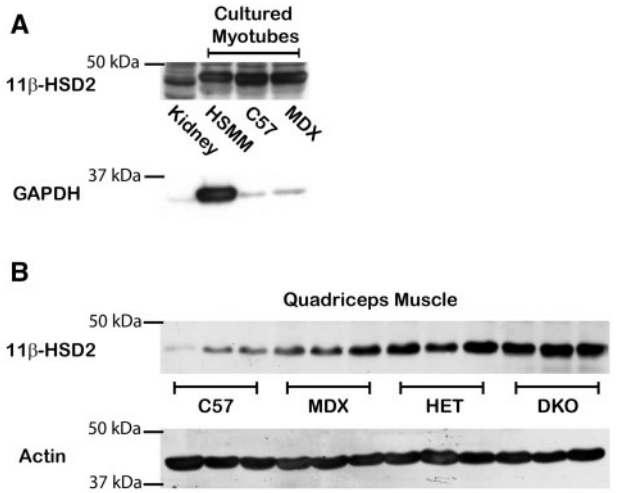

Figure 1. 11β-HSD2 is present in both human and mouse cultured myotubes and is increased in dystrophic skeletal muscle tissues. (**A**) 11β-HSD2 (44 kDa) was detected by western blots of human primary skeletal muscle (HSMM), C57/BL10 (C57), and *mdx* (MDX) myotubes differentiated for 5 days using equivalent amounts (35 μg) of cell lysates. Kidney is shown as a positive control tissue. GAPDH (36 kDa) shows equivalent loading of samples between C57 and MDX. (**B**) Representative western blot of quadriceps muscles from 3 biological replicates shows 11β-HSD2 protein levels from equivalent amounts (50 μg) of protein homogenates from: C57BL/10 wild-type control mice (C57), dystrophin-deficient *mdx* mice (MDX), dystrophin-deficient; utrophin haplo-insufficient mice (HET), and dystrophin/utrophin-deficient double knockout mice (DKO). Alpha-sarcomeric actin antibody (42 kDa) was used as a loading control.

11β-HSD2 is present in skeletal muscle. Western blot analysis revealed 11β-HSD2 is present in cultured mouse and human myotubes (Fig. 1A). Expression of 11β-HSD2 was confirmed by detection of RT-PCR products (Fig. 2) that were sequence verified (data not shown).

Previous studies have shown that inducing stress through hypoxia, shear stress, tumour necrosis factor alpha or angiotensin II can down-regulate or impair 11β-HSD2 expression (28–31). Since dystrophic muscle is under chronic mechanical and oxidative stress (32) we compared 11β-HSD2 protein levels in normal and dystrophic muscle tissues. Surprisingly, we found that 11β-HSD2 is increased in dystrophic skeletal muscle tissues compared to muscles from wild-type C57 control mice (Fig. 1B). 11β-HSD2 protein levels correlate with increasing disease severity in three mouse models of DMD: dystrophin-deficient *mdx;* dystrophin-deficient, utrophin-haploinsufficient (het); and dystrophin/utrophin-deficient (dko) mice (Fig. 1B). These data suggest that MR is protected from glucocorticoid binding in dystrophic muscle by increased 11β-HSD2 levels.

Circulating corticosteroid levels are not elevated in dystrophic mice

Since glucocorticoids are secreted in response to stress, we next tested whether circulating glucocorticoid levels were increased in dystrophic muscles. We measured the protein levels of the enzymes that catalyze the final and rate limiting step in the synthesis of corticosteroids (mineralocorticoids and glucocorticoids) in the adrenal glands from wild-type and dystrophic mice since the levels of these enzymes often reflect hormone levels (33–35). Neither CYP11B1 (Supplementary Material, Fig. S1A), the key enzyme in glucocorticoid (cortisol and corticosterone)

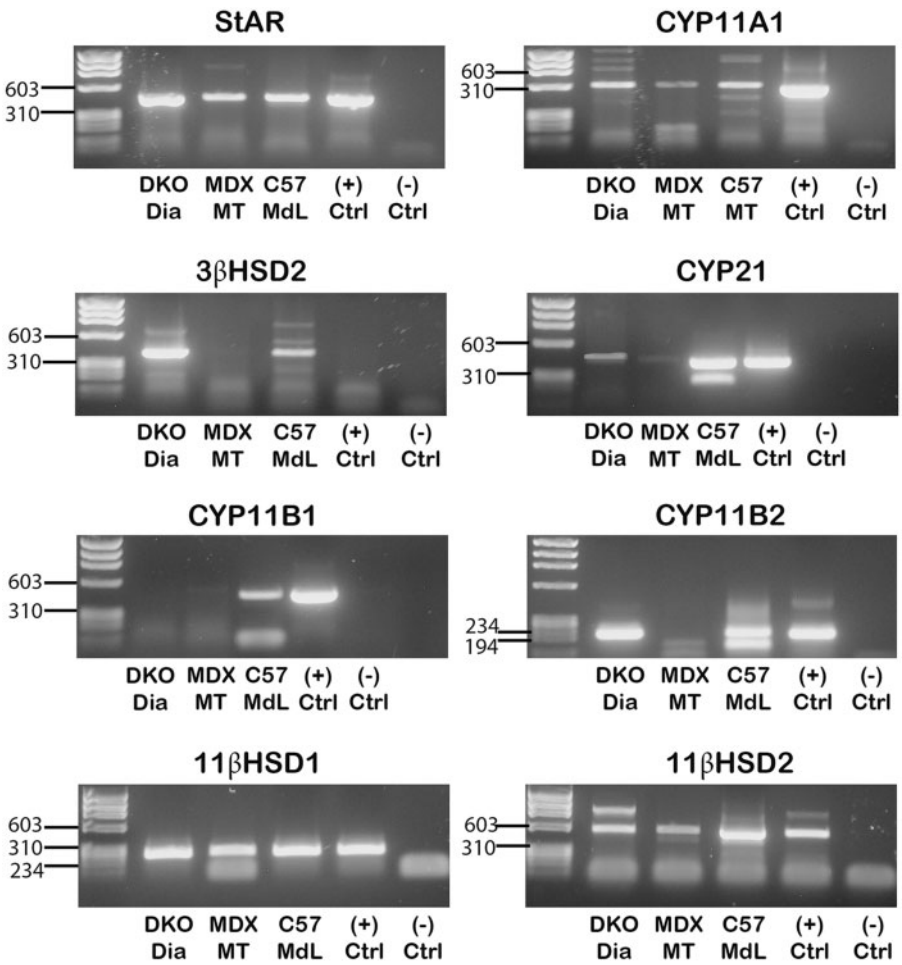

Figure 2. Detection of RT-PCR products verified the presence of enzymes required for aldosterone synthesis in muscle-derived leukocytes and dystrophic skeletal muscle tissue. RT-PCR products of transcripts encoding enzymes in the aldosterone synthesis pathway: StAR, CYP11A1, 3β-HSD2, CYP21, CYP11B1, CYP11B2, 11β-HSD1 and 11β-HSD2 from RNA isolated from DKO diaphragm muscle tissue (DKO Dia), differentiated myotubes from *mdx* primary myogenic cultures (MDX MT), and muscle-derived leukocytes isolated from C57 mice (C57 MdL). Only CYP11A1, StAR, 11β-HSD1 and 11β-HSD2 were detected in cultured mouse myotubes. CYP11B1 protein was detected in dystrophic skeletal muscle tissue but transcript levels were too low to verify expression. RNA isolated from an adrenal gland was used as a positive control for each PCR reaction. RT-PCR products were purified and sequenced. Sequences (not shown) were aligned to NCBI BLAST assembled genomes for confirmation of nucleic acid identity.

synthesis, nor CYP11B2 (aldosterone synthase) (Supplementary Material, Fig. S1B), the key enzyme in mineralocorticoid (aldosterone) synthesis is increased in the adrenal glands from dystrophic mice. Baseline serum or plasma levels, for cortisol and aldosterone respectively, confirmed that aldosterone and cortisol are not elevated in dystrophic het mice compared to wild-type (Supplementary Material, Fig. S1C). These data do not support the potential for excessive MR activation in dystrophic mice due to high circulating corticosteroid levels.

Presence of CYP11B1 and CYP11B2 in skeletal muscles suggests potential for local synthesis of aldosterone

Mineralocorticoids and glucocorticoids synthesized *de novo* have been shown to locally regulate steroid hormone receptors (21). To determine whether extra-adrenal synthesis of corticosteroids is possible in skeletal muscles, we first investigated whether the key enzymes CYP11B1 and CYP11B2 were present in skeletal muscle tissues. We demonstrated that CYP11B1 and CYP11B2 are present in skeletal muscle tissue homogenates by western blot analysis (Fig. 3A and B). As expected, protein levels of both enzymes are relatively low in normal, healthy skeletal muscle tissues compared to the adrenal positive control.

CYP11B2 protein levels are increased in dystrophic muscles

Since local synthesis can create high corticosteroid concentrations, particularly in pathological states (18–22), we examined whether CYP11B1 and CYP11B2 protein levels were increased in dystrophic muscle tissues compared to healthy controls. CYP11B2 is present at higher levels in all dystrophic muscle tissues examined compared to wild-type controls (Fig. 4A) in the three DMD mouse models tested (Supplementary Material, Fig. S2). CYP11B1 is not increased in dystrophic muscle tissues (Fig. 4B) compared to wild-type controls. CYP11B2 expression was confirmed in dystrophic muscle tissue by detection of RT-PCR products (Fig. 2) that were sequence verified (data not shown). However, CYP11B1 transcript levels are still too low in dystrophic muscle to confirm expression (Fig. 2). Increased CYP11B2

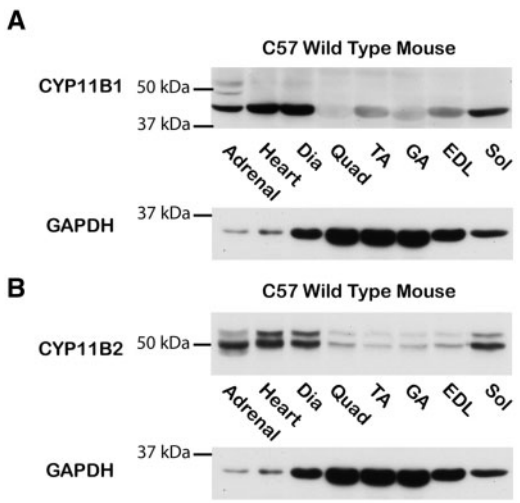

Figure 3. CYP11B1 and CYP11B2 protein are present in normal healthy skeletal muscle tissues. Representative western blots of (**A**) CYP11B1 and (**B**) CYP11B2 protein levels from equivalent amounts of protein homogenates from C57 mouse heart, diaphragm, quadriceps, *tibialis anterior*, gastrocnemius, *extensor digitorum longus*, and soleus muscles. 50 μg of total protein was loaded for all lanes and standardization of loading was verified using an anti-GAPDH antibody (36 kDa). Adrenal glands were included as positive controls and standardization of loading was verified using an anti-GAPDH antibody. Skeletal muscles were abbreviated as follows: Dia= diaphragm, Quad= quadriceps, TA= *Tibialis Anterior*, GA= gastrocnemius, EDL= *Extensor digitorum longus* and Sol= soleus.

levels in dystrophic muscles support the potential for high local aldosterone levels. CYP11B1 protein levels are consistently low in wild-type and dystrophic muscles, providing no evidence for increased local glucocorticoid levels.

CYP11B2 localizes to muscle-derived myeloid cells from the inflammatory response in dystrophic muscles

We tested whether CYP11B2 was present in cultured muscle myotubes. Western blot analysis of cultured myotubes revealed CYP11B2 is not present in normal human or mouse (C57 wild-type and *mdx*) myotubes under basal conditions. We attempted to induce myotubes to produce CYP11B2 with reagents known to increase CYP11B2 transcription in adrenal cells or cardiomyocytes including: angiotensin II, potassium, or glucose, but CYP11B2 protein and transcripts are not detectable after any of these treatments (Supplementary Material, Figs. S3A and B,2) in any of the muscle cultures.

Immunofluorescence staining of quadriceps muscles from wild-type and dystrophic mice revealed CYP11B2 localizes to areas of damage and does not appear to localize to muscle fibres (Fig. 5A). Numerous co-stains were conducted to identify the cell population producing CYP11B2. CYP11B2 co-localizes with a subset of CD11b-positive immune cells (Fig. 5B). Because CD11b is expressed by several leukocyte populations, we isolated leukocytes from normal (C57) and dystrophic (*mdx*) mouse limb muscles for analysis. *Mdx* mice were used for these studies because the timeline of inflammation in their skeletal muscles has been well-characterized, and it was important to analyze muscle tissues when infiltrating immune cell populations were elevated. Western blot analysis and detection of RT-PCR products confirmed that CYP11B2 protein and mRNA are present in muscle-derived leukocytes and are increased in leukocytes isolated from dystrophic muscle compared to wild-type (Figs. 2 and 5C). Immunofluorescence analysis showed localization of CYP11B2 protein in a higher percentage of myeloid cells from *mdx* muscle (35.7% ± 12.32%) compared to wild-type (10.90% ± 1.84%). CYP11B2 protein also appeared more densely distributed in myeloid cells isolated from *mdx* muscle compared to wild-type (Fig. 5D). Based on cell size and morphology, CYP11B2 protein does not appear to localize to lymphocytes, which are smaller than myeloid cells.

CYP11B2 is present in infiltrating immune cells that are elevated in dystrophic muscle due to ongoing muscle degeneration and inflammation. To determine whether increased CYP11B2 protein levels in dystrophic muscle led to higher aldosterone levels, we extracted aldosterone from the quadriceps and diaphragm muscles from C57 and *mdx* mice. Aldosterone levels are significantly higher in dystrophic quadriceps ($P = 0.02$) and diaphragm ($P = 0.05$) muscles from *mdx* mice compared to wild-type (Fig. 6A) even though circulating aldosterone levels in *mdx* mice are not increased compared to wild-type (Fig. 6B). Together, these data suggest that infiltrating myeloid cells may increase local aldosterone levels that could inappropriately activate MR and potentially exacerbate muscle damage.

Enzymes required for local aldosterone synthesis are present in muscle-derived leukocytes

To determine if aldosterone could be fully synthesized within skeletal muscle tissue or just metabolized from circulating precursors, we investigated whether the upstream enzymes required for aldosterone synthesis were present in skeletal muscle tissue homogenates, cultured myotubes and leukocytes isolated from skeletal muscle (Fig. 7). Detection of RT-PCR products confirmed that all enzymes in the pathway for aldosterone synthesis: StAR, CYP11A1, 3β-HSD2, CYP21, CYP11B1 and CYP11B2 are present in muscle derived leukocytes and dystrophic whole muscle homogenates, except for CYP11B1, which was confirmed only in muscle derived leukocytes (Figs. 2, 3 and 7). However, only the initial enzymes in the pathway: StAR and CYP11A1, which are required for all hormone synthesis, are present in cultured myotubes (Figs. 2 and 7). These data support that muscle-derived leukocytes express the transcripts for the enzymes required to locally synthesize aldosterone within dystrophic skeletal muscle tissue but not in skeletal muscle fibres themselves.

11β-HSD2, the tissue-specific enzyme regulating MR selectivity and its ubiquitously expressed counterpart 11β-HSD1, which converts inactive metabolites back to active glucocorticoids, are both present in muscle derived leukocytes, dystrophic tissue and cultured myotubes (Figs. 1 and 2). Presence of 11β-HSD2 supports that MR in both leukocytes and skeletal muscle fibres are aldosterone selective.

Discussion

Inflammation contributes to the pathology of Duchenne muscular dystrophy (DMD). This study is the first demonstration that an immune response is capable of producing aldosterone locally in damaged tissues where MR can be over-activated and lead to a detrimental gene expression profile that may exacerbate the damage. We have previously shown aldosterone treatment of normal human skeletal muscle myotubes upregulates detrimental genes associated with oxidative stress and other markers of diseased muscle, and that many of these genes are decreased by spironolactone (11). Similar results were seen in

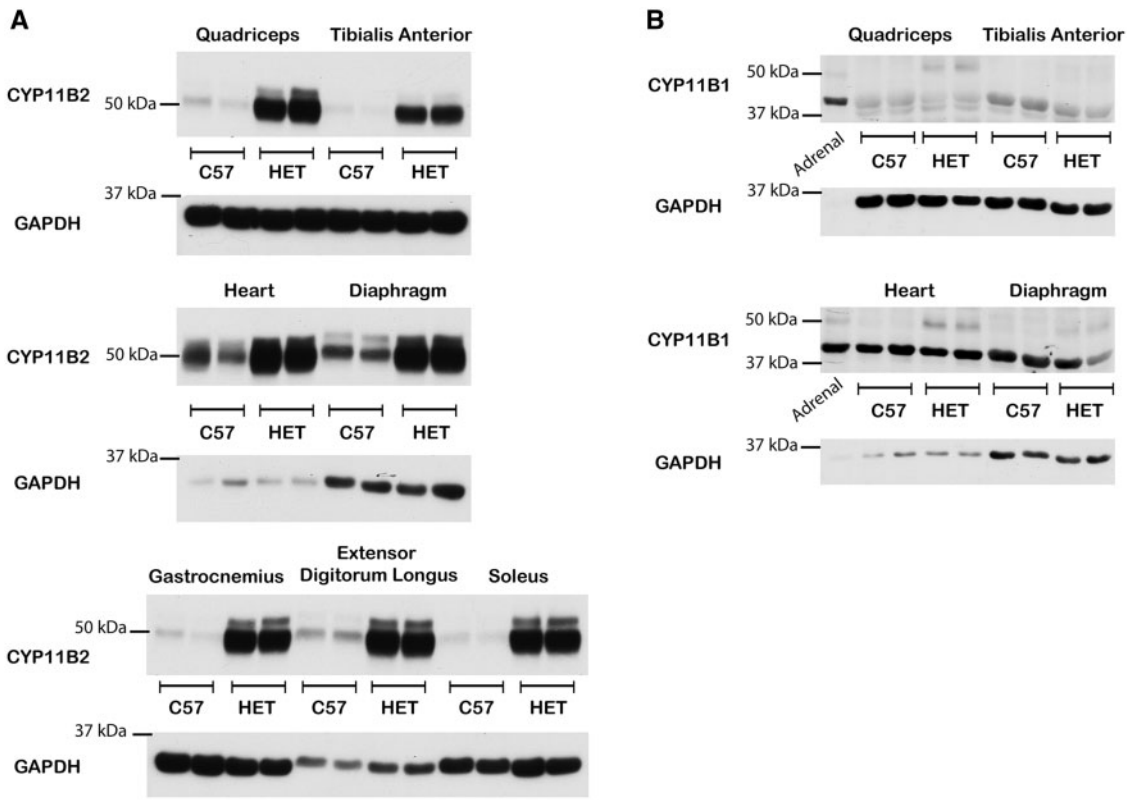

Figure 4. CYP11B2, but not CYP11B1 protein levels are increased in dystrophic skeletal muscle tissues compared to wild-type. Representative western blots of (**A**) CYP11B2 protein levels from equivalent amounts of protein homogenates from C57 and HET mouse: quadriceps, *tibialis anterior*, heart, diaphragm, gastrocnemius, *extensor digitorum longus* and soleus muscles; (**B**) CYP11B1 protein levels from equivalent amounts of protein homogenates from C57 and HET mouse: quadriceps, *tibialis anterior*, heart, and diaphragm muscles from 2 biological replicates. 50 μg of total protein was loaded for all lanes and standardization of loading was verified using an anti-GAPDH antibody (36 kDa). Adrenal glands were included as positive controls.

other studies that demonstrated spironolactone prevents aldosterone-induced inflammation and oxidative stress in the heart and hypothesized spironolactone may prevent oxidative stress associated with cardiac muscle wasting (36,37). Furthermore, we have found that long-term treatment with lisinopril and the mineralocorticoid receptor (MR) antagonist spironolactone improves the gene expression profile in dystrophic mouse skeletal muscle (11).

We show 11β-HSD2 is present in both mouse and human skeletal muscle fibres supporting that skeletal muscle is an aldosterone selective tissue. 11β-HSD2 protein levels are increased in dystrophic skeletal muscle homogenates compared to wild-type but are unchanged in normal and dystrophic cultured myotubes. 11β-HSD2 is typically unchanged or decreased in response to stress since it converts glucocorticoids to inactive metabolites, which can limit glucocorticoid receptor activity important for stress response (38). Since sequencing of RT-PCR products confirmed that 11β-HSD2 is also expressed in leukocytes isolated from skeletal muscle, 11β-HSD2 protein levels could be increased in dystrophic skeletal muscle homogenates because leukocyte populations are elevated in dystrophic muscle tissue. Alternatively, increased 11β-HSD2 protein levels could be coming from the muscle fibres themselves as a response to the microenvironment, which is lacking in cultured myotubes. Future studies measuring 11β-HSD2 levels in young dystrophic mice, prior to the onset of pathology, may help to begin to identify the signals responsible for its induction.

We show that CYP11B2 is expressed by muscle-derived myeloid cells that are elevated in dystrophic skeletal muscle tissue due to increased inflammation in areas of muscle degeneration. Based on cell size and morphology it appears the vast majority of CYP11B2 positive cells are monocytes or macrophages. Neutrophils isolated from *mdx* muscles appear to express the highest levels of CYP11B2, although they comprise a minor fraction of the myeloid cell population. CYP11B2 did not appear to be present in lymphoid cells isolated from *mdx* or wild-type muscles. Previous studies have shown that macrophages promote damage in dystrophic *mdx* mice and that decreasing neutrophil numbers in *mdx* mice reduces pathology (39,40). Macrophage-mediated damage has been attributed in part to iNOS-derived nitric oxide produced by M1 macrophages, but overall very little is known about the mechanisms through which myeloid cells promote pathology in *mdx* dystrophy. Our data demonstrate that myeloid cells isolated from *mdx* skeletal muscle are capable of producing aldosterone locally and identifies a new potential mechanism for myeloid cell-mediated pathology in DMD. Since MR regulate macrophage polarization (41), local aldosterone may exacerbate damage in dystrophic muscle by activating MR in macrophages to promote an M1 pro-inflammatory phenotype. Future studies with sorted muscle derived leukocytes will be needed to confirm the immune cell population(s) expressing high levels of CYP11B2.

Aldosterone levels were significantly higher in dystrophic skeletal muscles compared to wild-type despite normal

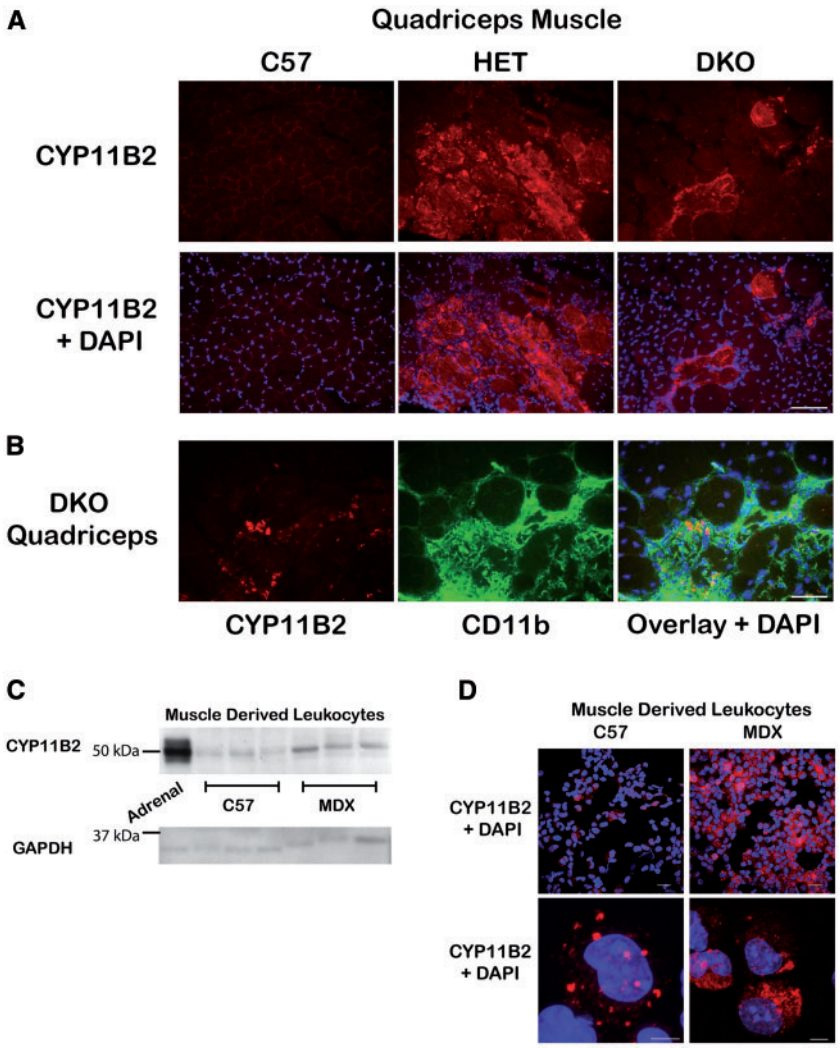

Figure 5. CYP11B2 is present at high levels in myeloid cells localized to areas of damage in dystrophic muscles. (**A**) CYP11B2 was detected in areas of damage within skeletal muscle tissue by immunofluorescence staining (red) of quadriceps muscle histological sections from C57 and dystrophic HET and DKO mice. Bar = 100 μm. (**B**) Immunofluorescence co-stain of CYP11B2 (red) and the immune cell marker CD11b (green) in quadriceps muscles from DKO mice revealed CYP11B2 co-localizes with a subset of CD11b-positive cells. The DNA dye DAPI is shown as a marker of nuclei (blue). Bar = 50 μm. (**C**) Western blot comparing CYP11B2 protein levels in myeloid cells isolated from hind limb musculature of C57 and MDX mice. CYP11B2 protein levels were lower compared to adrenal positive control and skeletal muscle tissue homogenates likely due to the series of enzymatic digestions and additional processing required to isolate leukocytes from skeletal muscles. Equivalent amounts (15 μg) of cell lysates were run with an adrenal gland sample included as a positive control. Standardization of loading was verified using an anti-GAPDH antibody. (**D**) CYP11B2 is present in a higher percentage of myeloid cells from MDX (35.7% ± 12.32%) muscle compared to C57 (10.90% ± 1.84%). CYP11B2 was detected by immunofluorescence staining (red) on C57 and MDX derived myeloid cells. Nuclei are stained with DAPI (blue). Top panel: confocal image without optical zoom, bar = 20 μm; and bottom panel: z-stack image of 0.22 μm optical slices, bar = 5 μm.

circulating aldosterone levels. Overall, aldosterone levels were 2.7 fold higher in dystrophic quadriceps muscle and 2.4 fold higher in dystrophic diaphragm muscle compared to wild-type. Since CYP11B2 protein levels were substantially increased in dystrophic muscle tissue and under normal conditions CYP11B2 is the rate-limiting enzyme in the aldosterone synthesis pathway, we anticipated a larger increase in aldosterone levels. However, we have found no evidence that other enzymes in the aldosterone synthesis pathway are increased and it is likely that aldosterone production is limited by another enzyme upstream of CYP11B2 or substrate availability in dystrophic muscle tissue. Also, local aldosterone has been shown to act in a paracrine manner on neighbouring cells, so even small increases can have a significant impact (42). Since aldosterone was extracted from whole skeletal muscle tissues, values obtained represent average aldosterone levels for the whole muscle. However, immunofluorescence staining revealed CYP11B2 is discretely localized to infiltrating leukocytes in areas of damage. Local production of aldosterone by these immune cells would be concentrated in damaged areas resulting in much higher localized concentrations compared to normal controls than the averages for the whole muscles. Aldosterone measurements will need to be repeated in the future in adrenalectomized mice to completely exclude the possibility that circulating aldosterone is being sequestered by the skeletal muscle.

Here, we demonstrate for the first time the presence of aldosterone synthesis enzymes in muscle-derived leukocytes and

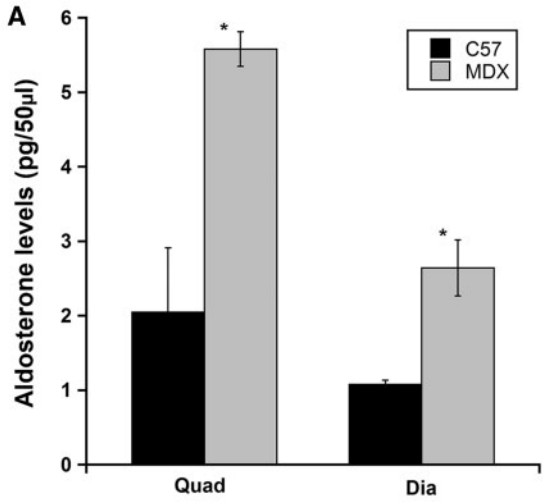

B

Mouse	Aldosterone (baseline)
C57-1	1304 pmol/L
C57-2	1352 pmol/L
C57-3	480 pmol/L
MDX-1	428 pmol/L
MDX-2	700 pmol/L
MDX-3	319 pmol/L

Figure 6. Aldosterone levels are significantly higher in dystrophic quadriceps and diaphragm muscles compared to wild-type, despite comparable circulating levels. (**A**) Aldosterone was extracted from quadriceps ($n=3$) and diaphragm ($n=2$) muscles from C57/BL10 wild-type mice (C57) and dystrophin-deficient *mdx* mice (MDX); samples were run in triplicate and assay was repeated with biological replicates to confirm results. Aldosterone concentrations are represented as mean value ± SEM. Student t-test was used to determine differences between C57 and MDX groups; *= quadriceps ($P=0.02$) and diaphragm ($P=0.05$). (**B**) Baseline plasma aldosterone levels are not increased in dystrophic mice compared to wild-type. Plasma was collected from age matched C57 ($n=6$) and MDX ($n=6$) mice.

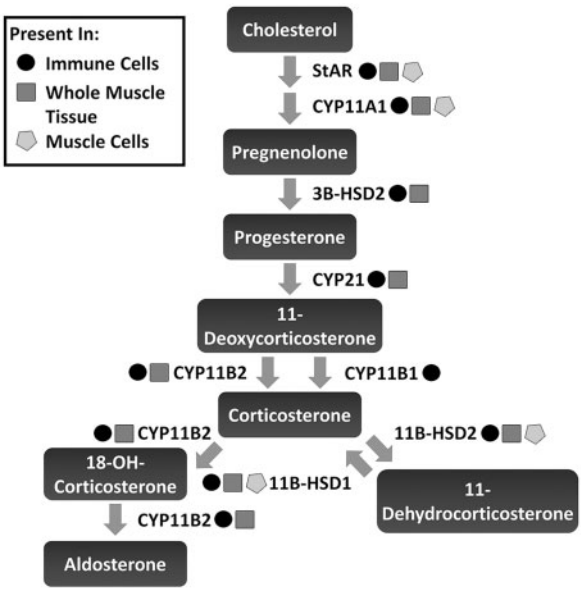

Figure 7. Enzymes necessary for local aldosterone synthesis are present in muscle-derived leukocytes. Schematic diagram depicting the aldosterone synthesis pathway and enzyme required for each step. Presence of each enzyme was confirmed by sequencing of RT-PCR products. Yellow star = detected in muscle cultures (myotubes generated from dystrophin-deficient *mdx* mouse neonatal myoblasts), green star = detected in immune cells (leukocytes isolated from C57BL/10 wild-type mice), and red star = detected in whole muscle tissue (diaphragm muscle tissue from dystrophin/utrophin-deficient double knockout dko mouse).

that CYP11B2 protein levels are greatly increased in myeloid cells isolated from dystrophic muscle compared to wild-type. Inflammation is a component of cardiac damage and heart failure, and blocking the activation of MR by locally synthesized aldosterone with MR antagonists may contribute to the efficacy seen in patients with normal circulating aldosterone levels, including those in the RALES and EPHESUS clinical trials. Since inflammation is a component of damage to many tissues and in many diseases, this study raises the possibility that MR antagonists may have therapeutic value in a wide variety of disorders where the target tissue expresses MR. Future studies will be needed to uncover the range of disorders to which our findings may have applicability and to identify the underlying mechanism leading to increased CYP11B2 expression in leukocytes.

Materials and Methods

Mice

All protocols were approved by the Institutional Laboratory Animal Care and Use Committee. Skeletal muscles, heart, adrenal glands, kidney and blood were removed from 8- to10-week-old dystrophin deficient *mdx*, dystrophin deficient utrophin haplo-insufficient (*utrn*$^{+/-}$; mdx) 'het' and dystrophin/utrophin-deficient double knockout 'dko' mice bred and genotyped as described previously (43) in addition to C57BL/10 (Harwell) wild-type controls.

Mammalian myogenic cell culture

Primary mouse myoblasts were isolated from neonatal C57BL/10 and *mdx* hind limb muscles through a series of collagenase digestions (collagenase type 2 from *Clostridium histolyticum*; Sigma). Endothelial cells were removed by size exclusion filtration through a 40 µm cell strainer (VWR), and the remaining cells were pre-plated on uncoated plastic dishes (Sigma) to remove fibroblasts. Primary cultures were grown in Nutrient Mixture F-10 HAM medium (Sigma) supplemented with 15% horse serum (HS; Invitrogen), 200 mM L-glutamine solution (Sigma), 200 mM calcium chloride (Sigma), 100 U/ml penicillin-streptomycin (Invitrogen) and 6 ng/ml basic human fibroblast growth factor (hBFGF; Sigma) and cultured at 37°C in 5% CO_2. To generate myotubes, myoblasts were serum restricted in differentiation media (F-10 HAM supplemented with 2% horse serum, 200 mM L-glutamine solution, 200 mM calcium chloride and 100 U/ml penicillin-streptomycin) for 24 h, after which, the horse serum was increased to 10% for another 4–5 days. Induced myotubes were treated 24–48 h with 16 mM potassium

chloride (KCl; Sigma) (44), 100 nM angiotensin II (Ang II; Sigma) (45) or 40 mM glucose (GLU; Sigma) (16). Cells were harvested in 200 μl cellular extract (CE) buffer as previously described (11).

Human skeletal muscle myoblasts isolated from normal males (HSMM, Lot #0000421209; Lonza) were grown in skeletal muscle cell growth medium (SkGM-2 bullet kit; Lonza) as previously described (11). Cells were serum restricted for 5 days in high glucose Dulbecco's modified medium (DMEM; Invitrogen), and supplemented with 2% HS and 100 U/ml penicillin-streptomycin. Induced myotubes were treated 24–48 h with KCl, Ang II or GLU and harvested in 200 μl of CE buffer.

Western blot analysis

Snap frozen mouse tissues were pulverized in liquid nitrogen and resuspended in cellular extract buffer as described previously (11). Briefly, tissue homogenates and cell lysates were sonicated on ice, centrifuged,and total protein was quantified (D_c Protein Assay, Biorad). 15–50 μg per lane of total protein from cell extracts or tissue homogenates were probed with a CYP11B1- or CYP11B2-specific mouse monoclonal antibody (46) or with antibodies against 11β-HSD2 (Cayman Chemical; #10004549), GAPDH (Proteintech; #10494-1-AP) and Actin (α-sarcomeric; Sigma; #A2172). Membranes were incubated with anti-mouse, rat, or rabbit HRP secondary antibodies (Jackson Immunoresearch) and signals were detected with ECL 2 western blotting substrate (Pierce) followed by film (blue ultra; GeneMate) exposure. GAPDH levels can vary between different tissues and in dystrophic mice due to metabolic dysfunction (47,48). However, several internal controls were tested (data not shown) and GAPDH was the most consistent control between samples.

Circulating baseline hormone level measurements

Following a sacrifice by cervical dislocation, blood was immediately extracted from mouse hearts and chest cavities. Blood was collected in hematology tubes (BD Microtainer), plasma samples were inverted immediately and centrifuged 10 min at 2000 x g while serum samples were allowed to clot for 30 min prior to centrifugation. Assays to measure baseline aldosterone and cortisol levels were performed by the Michigan State University Center for Population Control and Animal Health. A minimum of 200 μl plasma was collected for the aldosterone baseline test and a minimum of 500 μl serum was used for the cortisol baseline test; if necessary serum or plasma from 2 age- and sex-matched mice from each genotype was combined to get enough. To limit variability due to hormone fluctuations, mice were sacrificed between 9 and 10 AM each day by the same individual.

DNA sequencing

RNA was isolated using TRIzol reagent (Life Technologies) and DNAse (RQ1; Promega) treated as previously described (11). cDNA was generated using the Reverse Transcriptase High Capacity cDNA Reverse Transcription kit (Applied Biosystems), according to the manufacturer's instructions and PCR was performed using an Applied Biosystems ProFlex PCR System, with primers designed spanning introns in the mouse sequences for: stAR (5'GAACGGGGACGAAGTGCTAA3' forward–5'GCCACCCCTTCAGGTCAAT3' reverse); CYP11A1 (GGATGC TGGAGGAGATCGTG – GGCAAAGCTAGCCACCTGTA); 3βHSD2x1 (ACAGACCAGAACCAGCCTTTCT – TCCTCAGGTACTGGG TGTCAA); CYP21A1 (GGCCGACCCCATATGCTAAA – TGGTC CCGACTCTCTTGGAT); CYP11B1 (TCCAGTCCTCTCCTC ACTTTCAGG – CACATTAGTTCTGTCTTCCCTCACG); CYP11B2 (GGCCTGAACGCTATATGCCT – TGGGCATCAAAACAAAGCGG); 11βHSD1 (CCAGCAAAGGGATTGGAAGAG – GCGAGGTCTGA GTGATGTGGTTTAG); 11βHSD2 (TGACCAAGGCAGAGGACATCAG – TGGCATCTACAACTGGGCTAAGG) and human 11βHSD2 (TCTGGTTTTGGCAAGGAGACG – CGCATCAGCAACTACTTCAT TGTG). PCR products were purified and sequenced by The Ohio State Nucleic Acid/Microarray Shared Resource. Sequences were aligned to NCBI BLAST assembled genomes for confirmation of nucleic acid identity.

Immunofluorescence

Mouse quadriceps muscles were embedded in optimal-cutting temperature (OCT) medium and frozen on liquid-nitrogen cooled isopentane. 8 μm cryosections were stained with polyclonal primary antibodies against 11β-HSD2 (Cayman Chemical), or CYP11B2 (46) with Alexa 555 anti-rabbit secondary antibody (Life Technologies) or co-stained with CYP11B2 and CD11b (BD Pharmingen; # 550282) primary antibodies with Alexa 555 anti-rabbit or Alexa 488 anti-mouse (Life Technologies) secondary antibodies. Samples were mounted using Vectashield mounting medium (Vector Labs) with 1 μl/ml DAPI and viewed using a Nikon Eclipse 800 microscope. Images were taken under a 20X objective using a SPOT RT slider digital camera and SPOT software.

For immunofluorescence staining of muscle-derived leukocytes, cells were cytospun to slides (3 min; 800 rpm) and fixed 10 min with 4% paraformaldehyde (Sigma). Cells were stained with a CYP11B2 polyclonal primary antibody (Gomez-Sanchez), Alexa 555 anti-rabbit secondary antibody and mounted using Vectashield mounting medium with 1 μl/ml DAPI. Confocal images were taken using a Nikon A1Rsi Resonant scanning inverted confocal microscope under a 60X oil-immersion objective with or without optical zoom. CYP11B2 positive cells were counted by an individual blinded to genotypes.

Leukocyte isolation

Muscle leukocytes were isolated using a modified version of a previously described procedure (49). Mice were anaesthetized with an intraperitoneal injection of pentobarbital at a dosage of 40–60 mg/kg (Vortech Pharmaceuticals). Following anaesthesia, a thoracotomy was performed, a catheter needle was inserted into the left ventricle and an incision was made into the right atrium for saline perfusion and flow through, respectively. Saline was perfused through the animal to exclude the contamination of non-muscle residing leukocytes. Because of the scarcity of leukocytes in wild-type muscle, the hind limb musculature of 5 C57BL/10J mice (Jackson Laboratory) was pooled together. *Mdx* hind limb musculature was processed and analysed individually. Hind limb muscles were minced and digested twice in serum free DMEM with 0.2 mg/ml collagenase P (Roche) and 20 μg/ml DNAse I (Roche) for 30 min at 37 °C with trituration every 10 min. Following digestion, cell preparations were sequentially filtered through 70- and 40-μm filter-baskets. The filtrate was underlaid with Histopaque-1077 (Sigma Aldrich) and centrifuged at ~2400 x g for 20 min at room temperature. Cells at the interface were harvested, counted and saved for subsequent analyses.

Aldosteroneextraction and ELISA

Aldosterone was extracted from C57BL/10J, *mdx* and het mouse quadriceps and diaphragm muscles using a modified version of a previously described procedure (50). Tissues were weighed, homogenized in 5 ml water using a Polytron homogenizer and extracted with 10 ml ethyl acetate (Sigma). Samples were mixed thoroughly and centrifuged 15 min; the organic layer was transferred to a clean tube and dried with air flow under the hood. Samples were reconstituted in 2 ml water, loaded onto a C18 column (PerkinElmer) and eluted with 2 ml methanol. Methanol was evaporated with a centrifugal evaporator and the sample was reconstituted in 200 μl ELISA buffer (20 mM sodium phosphate (Sigma), 100 mM sodium chloride (Sigma), 0.01% thimerosal (Sigma), 0.05% tween (Sigma) and 0.5% bovine serum albumin (Fischer Scientific). Total protein recovered was measured using a Nanodrop 2000C.

Aldosterone was measured by ELISA using a specific monoclonal antibody and protocol previously developed and published (50–52). Briefly, a high binding 96-well plate (Thermo Scientific) was coated with Mouse Gamma Globulin (Jackson ImmunoResearch) and incubated overnight at 4 °C. For this competition ELISA plates were incubated with a goat anti-mouse antibody (Lampire) and Aldo A2E11 Integra antibody (51) prior to adding the samples and aldosterone standards. Samples and aldosterone standards (8 standards ranging from 0 to 25 pg/50 μl) were plated in triplicate and incubated with an aldo-3CMO-xx-biotin secondary antibody (52) followed by Avidin HRP. Samples were visualized using a colormetric TMB ELISA substrate solution (Thermo Fisher) and stopped with sulphuric acid (Sigma); plates were read at 450 nm with a BioTek Power Wave XS plate reader. A student *t*-test was used to determine differences between the two groups when appropriate. Summary values are presented as mean ± SEM and P-value ≤ 0.05 was considered statistically significant.

Supplementary Material

Supplementary Material is available at *HMG* online.

Acknowledgements

We thank Sara Cole and The Ohio State University Campus Microscopy & Imaging Facility for assistance with confocal imaging, Neha Rastogi for blinded quantification, and The Ohio State University Genomics Shared Resource for conducting DNA sequencing.

Conflict of Interest statement. None declared.

Funding

This work was supported by National Institutes of Health [R01 NS082868 and R01 HL116533 to JRF, R01 AR062579 to JGT, and F32 AR065845 to SSW]; and Department of Defense [MD120063 to JRF].

References

1. Mendell, J.R., Shilling, C., Leslie, N.D., Flanigan, K.M., al-Dahhak, R., Gastier-Foster, J., Kneile, K., Dunn, D.M., Duval, B., Aoyagi, A., *et al*. (2012) Evidence-based path to newborn screening for Duchenne muscular dystrophy. *Ann. Neurol.*, **71**, 304–313.
2. Guiraud, S., Aartsma-Rus, A., Vieira, N.M., Davies, K.E., van Ommen, G.J. and Kunkel, L.M. (2015) The Pathogenesis and Therapy of Muscular Dystrophies. *Annu. Rev. Genomics Hum. Genet.*, **16**, 281–308.
3. Rafael-Fortney, J.A., Chimanji, N.S., Schill, K.E., Martin, C.D., Murray, J.D., Ganguly, R., Stangland, J.E., Tran, T., Xu, Y., Canan, B.D., *et al*. (2011) Early treatment with lisinopril and spironolactone preserves cardiac and skeletal muscle in Duchenne muscular dystrophy mice. *Circulation*, **124**, 582–588.
4. Evans, R.M. (1988) The steroid and thyroid hormone receptor superfamily. *Science*, **240**, 889–895.
5. Yang, J. and Young, M.J. (2009) The mineralocorticoid receptor and its coregulators. *J. Mol. Endocrinol.*, **43**, 53–64.
6. Hawkins, U.A., Gomez-Sanchez, E.P., Gomez-Sanchez, C.M., and Gomez-Sanchez, C.E. (2012) The ubiquitous mineralocorticoid receptor: clinical implications. *Curr. Hypertens. Rep.*, **14**, 573–580.
7. Odermatt, A. and Kratschmar, D.V. (2012) Tissue-specific modulation of mineralocorticoid receptor function by 11beta-hydroxysteroid dehydrogenases: an overview. *Mol. Cell. Endocrinol.*, **350**, 168–186.
8. Rogerson, F.M., Yao, Y., Smith, B.J. and Fuller, P.J. (2004) Differences in the determinants of eplerenone, spironolactone and aldosterone binding to the mineralocorticoid receptor. *Clin. Exp. Pharmacol. Physiol.*, **31**, 704–709.
9. Tamargo, J., Solini, A. and Ruilope, L.M. (2014) Comparison of agents that affect aldosterone action. *Semin. Nephrol.*, **34**, 285–306.
10. Lowe, J., Wodarcyk, A.J., Floyd, K.T., Rastogi, N., Schultz, E.J., Swager, S.A., Chadwick, J.A., Tran, T., Raman, S.V., Janssen, P.M., *et al*. (2015) The angiotensin converting enzyme inhibitor lisinopril improves muscle histopathology but not contractile function in a mouse model of Duchenne muscular dystrophy. *J. Neuromuscul. Dis.*, **2**, 257–268.
11. Chadwick, J.A., Hauck, J.S., Lowe, J., Shaw, J.J., Guttridge, D.C., Gomez-Sanchez, C.E., Gomez-Sanchez, E.P. and Rafael-Fortney, J.A. (2015) Mineralocorticoid receptors are present in skeletal muscle and represent a potential therapeutic target. *FASEB J.*, **29**, 4544–4554.
12. Pitt, B., Remme, W., Zannad, F., Neaton, J., Martinez, F., Roniker, B., Bittman, R., Hurley, S., Kleiman, J. and Gatlin, M. (2003) Eplerenone, a selective aldosterone blocker, in patients with left ventricular dysfunction after myocardial infarction. *N. Engl. J. Med.*, **348**, 1309–1321.
13. Pitt, B., Zannad, F., Remme, W.J., Cody, R., Castaigne, A., Perez, A., Palensky, J. and Wittes, J. (1999) The effect of spironolactone on morbidity and mortality in patients with severe heart failure. *N. Engl. J. Med.*, **341**, 709–717.
14. Funder, J.W. (2007) The role of aldosterone and mineralocorticoid receptors in cardiovascular disease. *Am. J. Cardiovasc. Drugs*, **7**, 151–157.
15. Lam, E.Y., Funder, J.W., Nikolic-Paterson, D.J., Fuller, P.J. and Young, M.J. (2006) Mineralocorticoid receptor blockade but not steroid withdrawal reverses renal fibrosis in deoxycorticosterone/salt rats. *Endocrinology*, **147**, 3623–3629.
16. Fujisaki, M., Nagoshi, T., Nishikawa, T., Date, T. and Yoshimura, M. (2013) Rapid induction of aldosterone synthesis in cultured neonatal rat cardiomyocytes under high glucose conditions. *Biomed. Res. Int.*, **2013**, 161396.
17. Gomez-Sanchez, E.P., Gomez-Sanchez, C.M., Plonczynski, M.,. and Gomez-Sanchez, C.E. (2010) Aldosterone synthesis in the brain contributes to Dahl salt-sensitive rat hypertension. *Exp. Physiol.*, **95**, 120–130.

18. Silvestre, J.S., Heymes, C., Oubenaissa, A., Robert, V., Aupetit-Faisant, B., Carayon, A., Swynghedauw, B. and Delcayre, C. (1999) Activation of cardiac aldosterone production in rat myocardial infarction: effect of angiotensin II receptor blockade and role in cardiac fibrosis. *Circulation*, **99**, 2694–2701.
19. Silvestre, J.S., Robert, V., Heymes, C., Aupetit-Faisant, B., Mouas, C., Moalic, J.M., Swynghedauw, B. and Delcayre, C. (1998) Myocardial production of aldosterone and corticosterone in the rat. Physiological regulation. *J. Biol. Chem.*, **273**, 4883–4891.
20. Rudolph, A.E., Blasi, E.R. and Delyani, J.A. (2000) Tissue-specific corticosteroidogenesis in the rat. *Mol. Cell. Endocrinol.*, **165**, 221–224.
21. Taves, M.D., Gomez-Sanchez, C.E. and Soma, K.K. (2011) Extra-adrenal glucocorticoids and mineralocorticoids: evidence for local synthesis, regulation, and function. *Am. J. Physiol. Endocrinol. Metab.*, **301**, E11–E24.
22. Young, M.J., Clyne, C.D., Cole, T.J. and Funder, J.W. (2001) Cardiac steroidogenesis in the normal and failing heart. *J. Clin. Endocrinol. Metab.*, **86**, 5121–5126.
23. Gomez-Sanchez, E.P., Ahmad, N., Romero, D.G.,. and Gomez-Sanchez, C.E. (2005) Is aldosterone synthesized within the rat brain?. *Am. J. Physiol. Endocrinol. Metab.*, **288**, E342–E346.
24. Mizuno, Y., Yoshimura, M., Yasue, H., Sakamoto, T., Ogawa, H., Kugiyama, K., Harada, E., Nakayama, M., Nakamura, S., Ito, T., *et al.* (2001) Aldosterone production is activated in failing ventricle in humans. *Circulation*, **103**, 72–77.
25. Yamamoto, N., Yasue, H., Mizuno, Y., Yoshimura, M., Fujii, H., Nakayama, M., Harada, E., Nakamura, S., Ito, T. and Ogawa, H. (2002) Aldosterone is produced from ventricles in patients with essential hypertension. *Hypertension*, **39**, 958–962.
26. Yoshimura, M., Nakamura, S., Ito, T., Nakayama, M., Harada, E., Mizuno, Y., Sakamoto, T., Yamamuro, M., Saito, Y., Nakao, K., *et al.* (2002) Expression of aldosterone synthase gene in failing human heart: quantitative analysis using modified real-time polymerase chain reaction. *J. Clin. Endocrinol. Metab.*, **87**, 3936–3940.
27. Ito, T., Yoshimura, M., Nakamura, S., Nakayama, M., Shimasaki, Y., Harada, E., Mizuno, Y., Yamamuro, M., Harada, M., Saito, Y., *et al.* (2003) Inhibitory effect of natriuretic peptides on aldosterone synthase gene expression in cultured neonatal rat cardiocytes. *Circulation*, **107**, 807–810.
28. Lanz, C.B., Causevic, M., Heiniger, C., Frey, F.J., Frey, B.M. and Mohaupt, M.G. (2001) Fluid Shear Stress Reduces 11ss-Hydroxysteroid Dehydrogenase Type 2. *Hypertension*, **37**, 160–169.
29. Lanz, B., Kadereit, B., Ernst, S., Shojaati, K., Causevic, M., Frey, B.M., Frey, F.J. and Mohaupt, M.G. (2003) Angiotensin II regulates 11beta-hydroxysteroid dehydrogenase type 2 via AT2 receptors. *Kidney Int.*, **64**, 970–977.
30. Frey, F.J. (2006) Impaired 11 beta-hydroxysteroid dehydrogenase contributes to renal sodium avidity in cirrhosis: hypothesis or fact?. *Hepatology*, **44**, 795–801.
31. Heiniger, C.D., Kostadinova, R.M., Rochat, M.K., Serra, A., Ferrari, P., Dick, B., Frey, B.M.,. and Frey, F.J. (2003) Hypoxia causes down-regulation of 11 beta-hydroxysteroid dehydrogenase type 2 by induction of Egr-1. *FASEB J.*, **17**, 917–919.
32. Dudley, R.W.R., Danialou, G., Govindaraju, K., Lands, L., Eidelman, D.H. and Petrof, B.J. (2006) Sarcolemmal Damage in Dystrophin Deficiency Is Modulated by Synergistic Interactions between Mechanical and Oxidative/Nitrosative Stresses. *Am. J. Pathol.*, **168**, 1276–1287.
33. Liakos, P., Lenz, D., Bernhardt, R., Feige, J.J. and Defaye, G. (2003) Transforming growth factor beta1 inhibits aldosterone and cortisol production in the human adrenocortical cell line NCI-H295R through inhibition of CYP11B1 and CYP11B2 expression. *J. Endocrinol.*, **176**, 69–82.
34. Cao, C., Yang, X., Li, L., Sun, R., Xian, Y., Lv, W., Wang, J., Xu, Y. and Gao, Y. (2011) Increased expression of CYP17 and CYP11B1 in subclinical Cushing's syndrome due to adrenal adenomas. *Int. J. Urol.*, **18**, 691–696.
35. Nanba, K., Tsuiki, M., Sawai, K., Mukai, K., Nishimoto, K., Usui, T., Tagami, T., Okuno, H., Yamamoto, T., Shimatsu, A., *et al.* (2013) Histopathological diagnosis of primary aldosteronism using CYP11B2 immunohistochemistry. *J. Clin. Endocrinol. Metab.*, **98**, 1567–1574.
36. Burniston, J.G., Saini, A., Tan, L.B. and Goldspink, D.F. (2005) Aldosterone induces myocyte apoptosis in the heart and skeletal muscles of rats in vivo. *J. Mol. Cell. Cardiol.*, **39**, 395–399.
37. Young, M.J. and Rickard, A.J. (2012) Mechanisms of mineralocorticoid salt-induced hypertension and cardiac fibrosis. *Mol. Cell. Endocrinol.*, **350**, 248–255.
38. Chapman, K., Holmes, M. and Seckl, J. (2013) 11β-hydroxysteroid dehydrogenases: intracellular gate-keepers of tissue glucocorticoid action. *Physiol. Rev.*, **93**, 1139–1206.
39. Hodgetts, S., Radley, H., Davies, M. and Grounds, M.D. (2006) Reduced necrosis of dystrophic muscle by depletion of host neutrophils, or blocking TNFalpha function with Etanercept in mdx mice. *Neuromuscul. Disord.*, **16**, 591–602.
40. Wehling, M., Spencer, M.J. and Tidball, J.G. (2001) A nitric oxide synthase transgene ameliorates muscular dystrophy in mdx mice. *J. Cell Biol.*, **155**, 123–131.
41. Bene, N.C., Alcaide, P., Wortis, H.H. and Jaffe, I.Z. (2014) Mineralocorticoid receptors in immune cells: emerging role in cardiovascular disease. *Steroids*, **91**, 38–45.
42. Pazirandeh, A., Xue, Y., Rafter, I., Sjovall, J., Jondal, M. and Okret, S. (1999) Paracrine glucocorticoid activity produced by mouse thymic epithelial cells. *FASEB J.*, **13**, 893–901.
43. Deconinck, A.E., Rafael, J.A., Skinner, J.A., Brown, S.C., Potter, A.C., Metzinger, L., Watt, D.J., Dickson, J.G., Tinsley, J.M. and Davies, K.E. (1997) Utrophin-dystrophin-deficient mice as a model for Duchenne muscular dystrophy. *Cell*, **90**, 717–727.
44. LeHoux, J.G. and Lefebvre, A. (1998) Transcriptional activity of the hamster CYP11B2 promoter in NCI-H295 cells stimulated by angiotensin II, potassium, forskolin and bisindolylmaleimide. *J. Mol. Endocrinol.*, **20**, 183–191.
45. Oki, K., Kopf, P.G., Campbell, W.B., Luis Lam, M., Yamazaki, T., Gomez-Sanchez, C.E.,. and Gomez-Sanchez, E.P. (2013) Angiotensin II and III metabolism and effects on steroid production in the HAC15 human adrenocortical cell line. *Endocrinology*, **154**, 214–221.
46. Gomez-Sanchez, C.E., Qi, X., Velarde-Miranda, C., Plonczynski, M.W., Parker, C.R., Rainey, W., Satoh, F., Maekawa, T., Nakamura, Y., Sasano, H., *et al.* (2014) Development of monoclonal antibodies against human CYP11B1 and CYP11B2. *Mol. Cell. Endocrinol.*, **383**, 111–117.
47. Barber, R.D., Harmer, D.W., Coleman, R.A. and Clark, B.J. (2005) GAPDH as a housekeeping gene: analysis of GAPDH mRNA expression in a panel of 72 human tissues. *Physiol. Genomics*, **21**, 389–395.
48. Pant, M., Sopariwala, D.H., Bal, N.C., Lowe, J., Delfin, D.A., Rafael-Fortney, J. and Periasamy, M. (2015) Metabolic dysfunction and altered mitochondrial dynamics in the utrophin-dystrophin deficient mouse model of duchenne muscular dystrophy. *PLoS One*, **10**, e0123875.

49. Villalta, S.A., Rosenthal, W., Martinez, L., Kaur, A., Sparwasser, T., Tidball, J.G., Margeta, M., Spencer, M.J. and Bluestone, J.A. (2014) Regulatory T cells suppress muscle inflammation and injury in muscular dystrophy. *Sci. Transl. Med*, **6**, 258ra142.
50. Gomez-Sanchez, E.P., Ahmad, N., Romero, D.G.,. and Gomez-Sanchez, C.E. (2004) Origin of aldosterone in the rat heart. *Endocrinology*, **145**, 4796–4802.
51. Gomez-Sanchez, C.E., Foecking, M.F., Ferris, M.W., Chavarri, M.R., Uribe, L.,. and Gomez-Sanchez, E.P. (1987) The production of monoclonal antibodies against aldosterone. *Steroids*, **49**, 581–587.
52. Gomez-Sanchez, C.E., Leon, L.M.,. and Gomez-Sanchez, E.P. (1992) Biotin-hydrazide derivatives for the development of steroid enzyme-linked immunoassays. *J. Steroid Biochem. Mol. Biol.*, **43**, 523–527.